Published in final edited form as:

Reproduction. 2021 April ; 161(4): 399–409. doi:10.1530/REP-20-0494.

Equine maternal aging affects oocyte lipid content, metabolic function and developmental potential

Giovana D Catandi[A], **Yusra M Obeidat**[B], **Corey D Broeckling**[C], **Thomas W Chen**[D], **Adam J Chicco**[E], **Elaine M Carnevale**[A,F]

[A]Equine Reproduction Laboratory, Department of Biomedical Sciences, Colorado State University, 3101 Rampart Road, Fort Collins, CO 80521, USA.

[B]Electronic Engineering Department, Hijjawi Faculty for Engineering Technology, Yarmouk University, Irbid, P.O. 21163, Jordan

[C]Proteomics and Metabolomics Facility, Colorado State University, Fort Collins, CO 80523, USA.

[D]Department of Electrical and Computer Engineering, Colorado State University, Fort Collins, CO 8523, USA.

[E]Department of Biomedical Sciences, Colorado State University, Fort Collins, CO 80523, USA.

Abstract

Advanced maternal age is associated with a decline in fertility and oocyte quality. We used novel metabolic microsensors to assess effects of mare age on single oocyte and embryo metabolic function, which has not yet been similarly investigated in mammalian species. We hypothesized that equine maternal aging affects the metabolic function of oocytes and in vitro-produced early embryos, oocyte mitochondrial DNA (mtDNA) copy number, and relative abundance of metabolites involved in energy metabolism in oocytes and cumulus cells. Samples were collected from preovulatory follicles from young (≤14 years) and old (≥20 years) mares. Relative abundance of metabolites in metaphase II oocytes (MII) and their respective cumulus cells, detected by liquid and gas chromatography coupled to mass spectrometry, revealed that free fatty acids were less abundant in oocytes and more abundant in cumulus cells from old versus young mares. Quantification of aerobic and anaerobic metabolism, respectively measured as oxygen consumption rate (OCR) and extracellular acidification rate (ECAR) in a microchamber containing oxygen and pH microsensors, demonstrated reduced metabolic function and capacity in oocytes and day-2 embryos originating from oocytes of old when compared to young mares. In mature oocytes, mtDNA was quantified by real-time PCR, was not different between the age groups and not indicative of mitochondrial function. Significantly more sperm-injected oocytes from young than old mares resulted in blastocysts. Our results demonstrate a decline in oocyte and embryo

[F]Corresponding author. elaine.carnevale@colostate.edu.

Author Contribution Statement

EC, AC and TC participated in study design, funding, and supervision of sensor experiments. EC obtained funding and supervised metabolomic experiment, and CB conducted assays. TC and YO developed and provided microsensors, and GC and YO performed microsensor assays. GC and EC performed mare procedures. GC analyzed data and prepared the manuscript, which was edited by EC, AC, CB, YO and TC.

Declaration of interest

The authors declare that there is no conflict of interest that could be perceived as prejudicing the impartiality of the research reported.

metabolic activity that potentially contributes to the impaired developmental competence and fertility in aged females.

Keywords

Age; Mare; Oocyte; Embryo; Metabolism

Introduction

Equine maternal aging is associated with reduced fertility, lower pregnancy rates, and more early pregnancy losses (Carnevale & Ginther, 1992; Carnevale et al., 2005; Morel et al., 2005; Allen et al., 2007). Multiple factors contribute to the impaired fertility associated with aging, such as uterine dysfunction (Carnevale & Ginther, 1992), reduced ovarian follicle numbers (Carnevale et al., 1993; Cuervo-Arango et al., 2019), and a decrease in oocyte quality (Carnevale & Ginther, 1995; Hendriks et al., 2015). In mares, maternal aging contributes to an increase in the incidence of altered oocyte morphology (Altermatt et al., 2009), spindle abnormalities and chromosome misalignment (Rizzo et al., 2018), as well as to a decline in mitochondrial DNA (mtDNA) copy numbers during maturation (Rambags et al., 2014; Campos-Chillon et al., 2015).

Mitochondria are the main providers of energy for cellular processes during oocyte maturation and early embryonic development through oxidative phosphorylation of adenosine diphosphate, utilizing substrates provided by cumulus cells (May-Panloup et al., 2007; Gardner & Wale, 2013). Oocyte mitochondrial content, estimated by mtDNA copy number, greatly increases during maturation (Hendriks et al., 2015; Lamas-Toranzo et al., 2018); then, mitochondrial replication arrests at early cleavage stages and restarts at blastocyst formation in equine embryos (Hendriks et al., 2019). Both mitochondrial content and activity in the oocyte are critical for successful early embryo development and can be indicators of developmental potential (Bentov et al., 2011). Alterations in mtDNA copy numbers have been related to developmental success, maternal age, and in vitro culture methods (Rambags et al., 2006; Kameyama et al., 2007; Diez-Juan et al., 2015; Hendriks et al., 2015; Pasquariello et al., 2019), although conflicting results and controversy still surround the topic (Viotti et al., 2017; Cecchino & Garcia-Velasco, 2019).

Mitochondrial function in oocytes and embryos has been described through a variety of methods, most of which are either invasive or require expensive equipment or a long time frame, making them unsuitable for clinical application (Sugimura et al., 2012; Rambags et al., 2014; Hashimoto et al., 2017; Pasquariello et al., 2019). Such methods are also limited in terms of data interpretation, as they do not provide actual quantification of mitochondrial activity. When studying intact cells, the best measure of mitochondrial function is the assessment of cellular respiration by quantification of oxygen consumption rate (OCR), qualified by the addition of distinct mitochondria inhibitors and uncouplers (Brand & Nicholls, 2011).

Clark-type oxygen sensors are electrochemical-based sensors capable of measuring changes in dissolved oxygen concentration from media containing biological samples and, therefore,

can be used for monitoring aerobic metabolism of single mammalian embryos and oocytes (Lopes et al., 2007; Tejera et al., 2011; Obeidat et al., 2018). Anaerobic glycolysis is routinely estimated through measurement of extracellular acidification rate (ECAR) of the surrounding media (TeSlaa & Teitell, 2014), as a proton co-exported from cells with lactate generated from anaerobic glycolysis is the main contributor to media acidification, despite some participation of other metabolic processes such as carbon dioxide production by the tricarboxylic acid (TCA) cycle (Mookerjee et al., 2015). Thus, the addition of a pH sensor in a microchamber containing the oxygen sensor allows estimation of both aerobic and anaerobic metabolism (Obeidat et al., 2019a).

Studies with human oocytes and embryos have reported positive correlations between OCR, embryonic development, and fertility outcomes (Tejera et al., 2011; Yamanaka et al., 2011; Hashimoto et al., 2017). However, effects of maternal aging on individual oocyte and embryo OCR and ECAR have not been assessed in any mammalian species. Additionally, the relationship between mitochondrial function measurements and mtDNA copy number has not been investigated in individual oocytes. The mare is a potential animal model to study maternal aging in women (Carnevale, 2008). We hypothesized that equine maternal aging impairs oocyte and early embryo metabolic parameters and function. Using microsensors, we assessed the metabolic function of individual metaphase II (MII) oocytes and intracytoplasmic sperm injection (ICSI)-produced early embryos. Functional endpoints were compared to oocyte mtDNA content. Oocytes and cumulus cells from similar age groups of mares were used to compare the relative abundance of metabolites, involved in energy metabolism and storage. Finally, oocytes were injected with sperm to determine the competence of oocytes from young and old mares to develop into blastocysts.

Materials and methods

Animals and experimental design

Colorado State University’s Institutional Animal Care and Use Committee approved all the procedures performed in this study. Samples were collected from similar groups of nonlactating mares of light-horse breeds, with some of the same mares used during three breeding seasons. For oocyte and cumulus cell metabolite quantification, samples were collected between June and August of 2016, from young mares [Young, 7-11 years (mean 10), n=8] and old mares [Old, 20-26 (mean 22.4), n=10]. For oocyte and early embryo metabolic assays, young mares [Young, 6-13 years (mean 9.3), n=7] and old mares [Old, 20-27 years (mean 23.9), n=8] were used for sample collections between June and August of 2018. Oocytes were collected from mares in 2018 and 2019 [Young, 6-14 years (mean 10.1), n=13; Old, 20-28 years (mean 24.4), n=11] to compare cleavage and blastocyst rates after ICSI; samples were collected between June and August. Mares were housed in dry lot paddocks with access to covered shelters and fed a mixture of grass and alfalfa hay; mineral salt and water were provided ad libitum. The experimental design was a prospective observational cohort study.

Oocyte collection and maturation

Mares' reproductive tracts were examined by transrectal ultrasonography with 7.5 MHz linear probe to assess ovarian activity. Follicular maturation was induced when a dominant follicle approximately 35 mm in diameter and endometrial edema indicative of estrus were observed. Human chorionic gonadotropin (2000 IU, intravenous; Chorulon, Merck Animal Health, Madison, NJ) and deslorelin acetate in an aqueous base (0.75 mg, intramuscular; Precision Pharmacy, Bakersfield, CA) were administered at 23±2 h (for metabolomics analyses) or 16±2 h (for metabolism assays and embryo production) before oocytes were collected by transvaginal, ultrasound-guided follicular aspiration of the dominant follicles or follicles, as described (Carnevale, 2016). Recovered cumulus oocyte complexes (COCs) were incubated in tissue culture media 199 with Earle's salts (GibcoTM, Thermo Fisher, Waltham, MA) with additions of 10% fetal calf serum, 25 μg/ml of gentamicin, and 0.2 mM pyruvate at 38.2°C in an atmosphere of 5% CO_2 and air for 19±2 h (metabolomic analyses of COCs) or 26±2 h (oocyte metabolic assays and ICSI). Oocyte maturation was considered complete at the time of oocyte use, approximately 42 h after the administration of induction drugs to mares, which is the timeline used for fertilization of equine oocytes from dominant follicles (Carnevale, 2016). After culture, oocytes were denuded of cumulus cells by sequential pipetting in a MOPS-buffered medium (G-MOPS™, Vitrolife, Englewood, CO) with 0.04% bovine serum albumin (BSA; Sigma-Aldrich, St Louis, MO) and hyaluronidase (200 IU/mL; Sigma-Aldrich) and evaluated to confirm complete removal of cumulus cells. Extrusion of the first polar body was confirmed. For electrochemical measurements of basal and maximal oxygen consumption rates (OCR) and extracellular acidification rates (ECAR), oocytes were placed in a MOPS-buffered medium (G-MOPS) with 0.04% BSA at 38.2°C until metabolism assays. For metabolomics analyses, individual oocytes and their respective cumulus cells were fixed separately in 50% methanol solution and stored in glass vials at −80°C until analyses.

Oocyte and cumulus cell metabolite extraction and detection using liquid and gas chromatography coupled to mass spectrometry

For the experiment, one set of samples (oocyte and corresponding cumulus cells) was collected per mare. Oocytes or cumulus cells, frozen individually at −80°C, were thawed to 4°C before the addition of 250 μL of 100% methanol. Samples were then sonicated in a QSonica ultrasonic processor at 65% amplitude for 10 min, before being vortexed for 2 h at 4°C. After centrifugation at 3000 x g at 4°C, two individual aliquots of 120 μL of extract were transferred into 2-mL glass vials and dried under nitrogen gas for mass spectrometry analyses by liquid chromatography (LC-MS) and gas chromatography (GC-MS). The number of cumulus cells per sample was not known, so the remaining pellet was used to estimate biomass through quantification of protein by reconstitution with urea and measurement of absorbance at 280 nm using a NanoDrop™ spectrophotometer (Thermo Fisher).

For LC-MS analysis, the cumulus cell extract was resuspended in volumes proportional to the protein content (5 μL of 100% methanol was used per 5 μg/μL of protein content) with a minimum volume of 25 μL. Oocyte samples had a protein concentration less than 5 μg/μL and were resuspended in 25 μL of 100% methanol. Two μL of the suspensions were injected

onto a ACQUITY UPLC system (Waters, Milford, MA) in randomized order and separated using a ACUITY UPLC CSH Phenyl Hexyl column (1.7 μM, 1.0 x 100 mm) (Waters), using a gradient from solvent A (A) (2 mM ammonium hydroxide, 0.1% formic acid) to solvent B (B) (99.9% acetonitrile, 0.1% formic acid). Injections were made in 100% A, held at 100% A for 1 min, ramped to 98% B over 12 min, held at 98% B for 3 min, and then returned to start conditions over 0.05 min and allowed to re-equilibrate for 3.95 min, with a 200 μL/min constant flow rate. The column and samples were held at 65°C and 6°C, respectively. The column eluent was infused into a Xevo G2 Q-TOF-MS (Waters) with an electrospray source in positive mode, scanning 50-2000 m/z at 0.2 s per scan, alternating between MS (6V collision energy) and MS^E mode (15-30V ramp). Calibration was performed using sodium iodide with 1 ppm mass accuracy. The capillary voltage was held at 2200 V, source temperature at 150°C, and nitrogen desolvation temperature at 350°C with a flow rate of 800 L/h.

For GC-MS analysis, the extract was resuspended in pyridine containing 25 mg/mL of methoxyamine hydrochloride (5 μL per 5 μg/μL of protein content for cumulus cells and 25 μL for oocytes), incubated at 60°C for 60 min, vigorously vortexed for 30 s, sonicated for 10 min, and incubated for an additional 60 min at 60°C. Additions of the same volume of N-methyl-N-trimethylsilyltrifluoroacetamide with 1% trimethylchlorosilane (MSTFA + 1% TMCS, Thermo Fisher) were made, and samples were vigorously vortexed for 30 s, then incubated at 60°C for 30 min. Metabolites were detected using a TRACE 1310 GC coupled to a ISQ™ mass spectrometer (ThermoFisher). One μL of the samples were injected at 10:1 split ratio to a 30 m TG-5MS column (Thermo Fisher, 0.25 mm i.d., 0.25 μm film thickness) with a 1.2 mL/min helium gas flow rate. The GC inlet was held at 285°C. The oven program started at 80°C for 30 s, followed by a ramp of 15°C/min to 330°C, and an 8 min hold. Masses between 50-650 m/z were scanned at 5 scans/s under electron impact ionization. Transfer line and ion source were held at 300 °C and 260°C, respectively.

For each sample, raw data files were converted to a computable document format (CDF), and matrix of molecular features, as defined by retention time and mass (m/z), was generated using XCMS in R software (BMC Bioinformatics) for feature detection and alignment (Smith et al., 2006). To account for the variance in cell numbers and protein content from cumulus cell samples, raw peak areas were first normalized to total protein in the sample. Oocyte samples were not normalized to protein content, as a constant volume was used for resuspension, and each sample contained a single cell. Peak areas were also subsequently quantile normalized in R. Outlier injections were detected based on total signal and PC1 of principle component analysis. Features were grouped using RAMClustR (Broeckling et al., 2014), which groups features into spectra based coelution and covariance across the full dataset, whereby spectra are used to determine the identity of observed compounds in the experiment. The peak areas for each feature in a spectrum were condensed via the weighted mean based on spectral matching to in-house, NISTv14, Golm, HMDB and LipidMaps 1-SToP libraries (Broeckling et al., 2016), and Metlin metabolite databases. For this study, we focused on interpretation of glucose, pyruvate, lactate and free fatty acids from the GC-MS data, as the primary energy substrates for oocyte maturation and early embryonic development. For LC-MS data, triglycerides (TG) composition was the focus of this study, as these are the main components of cellular energy storage.

In vitro embryo production

Prior to ICSI, oocytes were collected, matured and denuded of cumulus cells as described above. Frozen-thawed sperm from a single ejaculate from one stallion were used for ICSI. Approximately one-tenth of a 0.25-mL straw of frozen semen was cut under liquid nitrogen and thawed by placing directly in 1mL of MOPS-buffered medium (G-MOPS) with 0.04% BSA at 38.2°C. Prior to injection, one sperm was selected and prepared for sperm injection as previously described (Altermatt et al., 2009). ICSI was performed in MOPS-buffered medium (G-MOPS) with 0.04% BSA using a micromanipulator (Narishige Group, Amityville, NY) and a piezo-driven injection system (Prime Tech, Japan), after which presumptive zygotes were placed into embryo culture medium (global®, LifeGlobal Group, Guilford, CT) in individual 30-μL droplets under paraffin oil (OVOIL™, Vitrolife) and incubated at 38.2°C in 5% O_2, 7% CO_2 and 88% N_2. At 2 days (44-56 h, mean of 51.5 h after ICSI), early embryos with normal morphology and 2 to 8 cells (mean of 4 cells) were used for the measurement of basal OCR and ECAR. Embryos followed for blastocyst development were moved at 5 days after ICSI into individual 30-μl droplets of a second culture medium (global® for Fertilization, LifeGlobal Group). Embryos were observed daily until formation of a blastocyst or degeneration.

Oocyte and early embryo OCR and ECAR assays

Metabolic analyses of oocytes and early embryos were performed using a microchamber with electrochemical-based oxygen and pH sensors previously described in detail (Obeidat et al., 2019a, b). One or two samples per mare were analyzed. Briefly, for each oocyte or early embryo assay, the microchamber was filled with 120 μL of MOPS-buffered medium (G-MOPS) with 0.04% BSA, overlaid with 120 μL of paraffin oil (OVOIL) to limit the chamber from atmospheric oxygen diffusion. The three-electrode oxygen sensor was connected to a potentiostat (Quadstat EA 164H, eDAQ Inc., Colorado Springs, CO) that applied voltage to the sensor and monitored the decrease in oxygen reduction current over time. The applied potential during all amperometric oxygen assays was set at −0.6V. The pH sensor was connected to a custom-made Ina333 instrumentation amplifier circuit that measured the change in voltage. The starting (room air saturated) oxygen concentration and pH of the medium was measured as baseline current for 2 min and calibrated as previously described in detail (Obeidat et al., 2019a). The rate of change in chamber oxygen and pH from baseline values over time (following addition of sample) were used for calculations of sample OCR and ECAR, respectively.

After measuring oxygen and pH baselines, individual oocytes or early embryos were transferred into the microchamber and placed on top of the oxygen sensor. Basal OCR was assayed for 5 min, followed by ECAR assessment for 2 min. To determine respiration related to proton leak and stimulate maximal ECAR, a subset of 10 oocytes (n=3 from Young, n=7 from Old) was exposed to 1 μM oligomycin, an ATP-synthase inhibitor; OCR was assessed for 5 min and ECAR for 2 min. Because oxygen consumption related to proton leak was so small, as previously demonstrated by our group (Obeidat et al., 2018), subsequent oocyte assays did not include the addition of oligomycin.

Our laboratory has validated that the maximal respiratory capacity of bovine oocytes can be achieved by titration of protonophore uncoupler agents (Obeidat et al., 2018). Three titrations of 1 μM carbonyl cyanide *m*-chlorophenyl hydrazone (CCCP, Sigma-Aldrich) were performed during the equine oocyte assays, each followed by OCR measurement for 5 min and ECAR for 2 min. Maximal OCR was defined as the highest stable value observed during CCCP titrations. After metabolic readings, individual oocytes were stored at −80°C for subsequent mitochondrial DNA (mtDNA) quantification.

Oocyte mitochondrial DNA content absolute quantification

Mitochondrial DNA (mtDNA) content of single oocytes (one or two samples per mare) was quantified by real-time PCR (qPCR) as previously described (Pasquariello et al., 2019) using kits and supplies from one source (Qiagen, German-town, MD) unless otherwise noted. Briefly, DNA extraction of individually cryopreserved oocytes was performed using the QIAamp DNA micro kit according to the manufacturer's protocol with carrier RNA (1 μg) added to each sample. The DNA sample was eluted with 50 μL of Buffer AE (supplied with the kit) and analyzed for RT-qPCR using an absolute quantification assay. To prepare quantification standards, a 1096 bp fragment of the I-rRNA region of equine mtDNA was amplified by PCR using the LongRange PCR kit and a primer pair (5'-AGCAATTTCGGTTGGGGTGA-3' and 5'-GCTCGGTTGGTTTCGGCTAA-3') designed using Primer-BLAST (NBCI), then purified using the Qiaquick PCR purification kit and cloned using the Qiagen PCR cloning kit. Plasmid DNA containing the amplified mtDNA fragment was purified from bacteria using the Qiaprep miniprep kit. A standard curve was generated by using seven tenfold serial dilutions (10^7 to 10 copies), and standard curve correlation coefficients were greater than 0.98. Real-time quantitative PCR using the primer pair 5'-ATGGTTTGTGCTACTGCTCG-3' and 5'-GCCCTAACCCTGGCCTTAAC-3', designed with Primer-BLAST (NCBI), was run in triplicate for each standard dilution and sample in 10-μL reactions using PowerUp SYBR Green master mix (Applied Biosystems, Foster City, CA), a LightCycler 480II (Roche Applied Science, Indianapolis, IN) and the program of amplification: 50°C for 2 min for the first cycle; 95°C for 2 min for the second cycle; 95°C for 15 s and 60°C for 1 min for 40 cycles; a melting curve was run to assess specificity of the primers. Samples and standard curve were run on the same plate. Copy numbers of mtDNA were generated from the equation of Ct value against copy number for the corresponding standard curve.

Statistical analyses

Statistical analyses were completed using GraphPad Prism 8.0.2 (GraphPad Software, Inc., San Diego, CA). Student's *t*-tests were used to compare oocyte and early embryo continuous data, including relative abundance of metabolites, OCR and ECAR. Mann-Whitney tests were used to compare metabolomics data that failed the Shapiro-Wilk test for normality. Fisher's exact tests were used to compare cleavage and blastocyst rates. For OCR and ECAR comparisons of different developmental stages (oocytes and embryos), one-way ANOVA was used, followed by a post-hoc Tukey's HSD to determine the source of any differences. Differences were considered significant at $P < 0.05$. Relative abundances of metabolites are presented in box plots (median, first and third quartiles) with whiskers from minimum to maximum values. The remaining results are presented as mean ± SEM.

Results

Effects of maternal age on oocyte and cumulus cell metabolite composition

Metaphase II oocytes and their respective cumulus cells from Young (n=8) and Old (n=10) were evaluated by LC-MS and GC-MS for metabolite composition. One sample was obtained per mare, with cumulus cells and oocytes obtained from the same follicle. Relative abundance of glucose, pyruvate and lactate were similar between the two age groups for oocytes (P≥0.6) and cumulus cells (P≥ 0.2; Figure 1A-F). Relative abundance of total FFA were greater in oocytes from Young than Old, respectively (P=0.048; Figure 1G), but not in cumulus cells (P=0.08; Figure 1H). Total abundance of TG in oocytes and cumulus cells were similar between Young and Old (P≥0.2; Figure 1I, 1J); the relative abundance of each TG identified via LC-MS is included in Supplementary Table 1.

Four FFA were identified in oocytes and cumulus cells (Figure 2A and 2B). Although only the relative abundance of palmitic acid (C16:0) was higher (P=0.05) in oocytes, the general tendency was for all of FFA to be numerically higher in oocytes from Young than Old (stearic acid, C18:0, P=0.06; oleic acid, C18:1, P=0.1; linoleic acid, C18:2, P=0.1; Figure 2A). In contrast, the normalized abundance of linoleic acid was higher (P=0.01) in cumulus cells of Old when compared to Young, with similar relationship observed for most other FFA (palmitic acid, P=0.07; stearic acid, P=0.6; oleic acid, P=0.1; Figure 2B).

Effects of maternal age on oocyte metabolic function and mtDNA copy number

Oocytes from Young (n=9) and Old (n=14) were assayed for OCR and ECAR. Basal OCR was higher for oocytes from Young (1.8 ± 0.2 fmolO_2/s/oocyte) than Old (1.4 ± 0.1 fmolO_2/s/oocyte, P=0.02; Figure 3A). Higher rates of maximal OCR were also expressed by oocytes from Young (2.7 ± 0.2 fmolO_2/s/oocyte) when compared to Old (2.1 ± 0.1 fmolO_2/s/oocyte, P=0.007; Figure 3B). Mitochondrial efficiency, calculated as basal OCR/maximal OCR, represents the proportion of maximal respiratory capacity that a cell utilizes during basal metabolism. Mitochondrial reserve capacity, calculated as maximal OCR – basal OCR, is an indicator of the cellular ability to respond to increased energy demands. Both parameters were similar between groups (P ≥0.4). Proton leak OCR, achieved after addition of oligomycin, was not different among oocytes from Young and Old (0.02 ± 0.01 and 0.01 ± 0.004 fmolO_2/s/oocyte, respectively, P=0.8; Figure 3C). No difference was noted in mtDNA copy number between oocytes from Young (n=10) and Old (n=13) (5.6 x 10^5 ± 0.4 x 10^5 and 6.2 x 10^5 ± 0.4 x 10^5, respectively, P=0.3; Figure 3D).

Basal ECAR, an estimation of anaerobic glycolysis, was higher for oocytes from Young (20.8 ± 1.7 mpH/min/oocyte) than Old (15 ± 1.6 mpH/min/oocyte, P=0.03; Figure 3E). Maximal ECAR, stimulated by addition of oligomycin, was also higher (P=0.006) for Young (27.8 ± 2.9 mpH/min/oocyte) compared to Old (18.1 ± 1.2 mpH/min/oocyte, P=0.006; Figure 3F). The basal rate of glycolysis relative to oxidative phosphorylation, expressed as the ECAR/OCR ratio, was not different between groups (P=0.7; Figure 3G), indicating no effect of maternal aging on the relative contributions of anaerobic and aerobic metabolism to oocyte energy supply.

Effects of maternal age on early embryo metabolic function

Basal OCR and ECAR were assessed in day-2 embryos from Young (n=8) and Old (n=10). Basal OCR was higher for embryos from Young (3.8 ± 0.1 fmolO_2/s/embryo) than Old (3.2 ± 0.2 fmolO_2/s/embryo, P=0.05; Figure 4A). Basal ECAR was similar between groups (36.9 ± 2.7, 38.5 ± 2.1 mpH/min/embryo, P=0.7; Figure 4B). The ECAR/OCR ratio was similar for embryos from Young and Old (P=0.1; Figure 4C).

Basal OCR in early embryos was consistently higher than basal and maximal OCR in oocytes from Young or Old (P≤0.0001; Figure 5A). Similarly, basal ECAR in embryos was higher than in oocytes from Young or Old (P≤0.0001; Figure 5B), consistent with an increase in energy demands from both anaerobic and aerobic pathways during early embryo development. Average cell numbers of the day-2 embryos were not different between Young and Old (4.4 ± 0.5, 5 ± 0.4 cells, P=0.4).

Effects of maternal age on embryo development after ICSI

The number of sperm-injected oocytes that cleaved into at least two cells at 1 or 2 days after ICSI was similar between groups (Young, 25/29, 86% and Old, 22/24, 92%; Figure 6); however, embryonic development to the blastocyst stage at day 7 or 8 after ICSI was greater (P=0.04) for Young than Old per sperm-injected oocyte (Young, 14/29, 48% and Old, 5/24, 21%; Figure 6) or per cleaved embryo (Young, 14/25, 56% and Old, 5/22, 23%).

Discussion

We evaluated equine oocytes and early embryos to determine the effects of maternal aging on their metabolism, as a potential cause of the age-associated reduction in oocyte developmental potential. Our study describes novel findings using a noninvasive technology to assess metabolism in individual oocytes and embryos and describes metabolic alterations related to maternal aging. To the best of our knowledge, effects of maternal aging on individual oocyte and early-embryo metabolic function, as quantified by OCR and ECAR, have not been demonstrated in any mammalian species. The present study indicates that equine maternal aging is associated with impaired oocyte metabolic function and capacity. Our findings suggest that not only do oocytes from old mares produce less energy under basal conditions, they are also not capable of as much energy output as oocytes from young mares. The cause and effects of altered oocyte metabolism in the old mare is still to be determined; however, the current study provides new insight into metabolic alterations associated with aging.

During follicular development and maturation, oocyte metabolism is highly dependent on the surrounding cumulus cells, which provide energy substrates to oocytes (Cecchino et al., 2018). Glycolysis is a major pathway for production of energy in the follicle (Dumesic et al., 2015). However, the oocyte has low capacity for glucose metabolism, thus cumulus cells actively uptake glucose from the follicular environment or culture media, metabolize it, and transport pyruvate and lactate to the oocyte via gap junctions (Su et al., 2009; Wang et al., 2012). Metabolite analyses of MII oocytes and their respective cumulus cells demonstrated no effect of maternal age on the relative abundance of glucose, pyruvate and lactate.

Oocytes also metabolize fatty acids for energy production through β-oxidation in mitochondria. This pathway is more important in species that have abundant lipids in their oocytes, such as bovine and porcine (Sturmey et al., 2009; Paczkowski et al., 2013). Likewise, equine oocytes have a large accumulation of lipids and use fatty acid metabolism during maturation (Pirro et al., 2014), suggesting a reliance on β-oxidation to meet energy demands. In the present study, the relative abundance of FFA did not significantly differ in cumulus cells from young and old mares; conversely, FFA was lower in old than young mare oocytes. Potentially, the transport of FFA from cumulus cells to the oocyte is impaired with maternal aging. Although larger molecules than carbohydrates, FFA are also transported from the cumulus cells to the oocyte through transzonal projections (TZPs) which extend through the zona pellucida (del Collado et al., 2017). These cellular connections typically remain intact until the final stages of meiotic maturation (Barrett & Albertini, 2010; Clarke, 2018). However, a reduction in TZPs occurs with maternal aging in mice (El-Hayek et al., 2018). While the abundance of TZPs has not been assessed in equine COCs, alterations in oocyte morphology in old mares are suggestive of an earlier breakdown of TZPs during maturation. Oocytes from old mares can have larger inner zona pellucida (ZP) and perivitelline space volumes despite similar ooplasm diameters (Altermatt et al., 2009). This suggests that oocytes from old mares may grow larger and then shrink from the ZP, potentially disrupting TZPs. Fatty acids in the oocyte also come from the breakdown of TG molecules stored in lipid droplets, which are a major source of energy reserve for early embryonic development (Sturmey et al., 2009; Dumesic et al., 2015). During maturation, lipid metabolism is stimulated in COCs and is beneficial to oocyte developmental competence (Dunning et al., 2014). Differences in the relative abundance of FFA in oocytes could also indicate reduced activity of lipases in COCs from old mares, which are needed to break down the TG into FFA. Lipase expression and activity were not assessed in this study. The proportion of different FFAs was similar among oocytes and cumulus cells from both age groups. These same FFAs, in different proportional contributions, have been reported to be major components in oocytes from other species, such as porcine, bovine and human (Dunning et al., 2014).

Aerobic production of energy by the oocyte is essential for the completion of important events associated with maturation and fertilization. One of the most energy intensive activities within the oocyte is the assembly and disassembly of microtubules for spindle formation during meiosis (Chappel, 2013). Spindle abnormalities during maturation are more frequent in oocytes from old than young mares (Carnevale et al., 2012; Rizzo et al., 2018, 2019). Energy production potential in individual oocytes is typically deduced from indirect static outcomes or group assays of pooled samples. In the present study, we were able to assess indices of aerobic and anaerobic energy production in individual oocytes and early embryos from young and old mares. We observed a reduction in the energy-producing capacity of mitochondria in oocytes from old mares, demonstrated by lower basal and maximal OCR compared to oocytes from young mares. These findings are in agreement with previous findings in oocytes associated with advanced female age that are suggestive of mitochondrial dysfunction, such as reduced ATP content (Iwata et al., 2011; Simsek-Duran et al., 2013), loss of mitochondria cristae and matrix density (Kushnir et al., 2012; Rambags et al., 2014), reduced mitochondrial membrane potential (Pasquariello et al., 2019), and

altered mtDNA copy numbers (Rambags et al., 2006, 2014; Campos-Chillon et al., 2015; Pasquariello et al., 2019). In a recent study, it was reported that most of the glucose metabolism in equine COCs results in the production of lactate, while the majority of ATP production is from fatty acid oxidation supported by the ooplasmic lipid reserve (Lewis et al., 2020). Therefore, the lower OCR observed in oocytes from old mares in the present study could reflect insufficient availability of FFA to meet ATP demands through oxidative metabolism.

Multiple events during oocyte cytoplasmic and nuclear maturation and embryonic development after fertilization are associated with anaerobic metabolism (Lamas-Toranzo et al., 2018). Advanced maternal age also impaired oocyte anaerobic glycolytic activity and capacity, which may be attributed to loss of enzymatic activity, since glucose and pyruvate availability were similar in oocytes from both age groups. Therefore, oocytes from old mares did not compensate for the lower energy production from aerobic metabolism by increasing glycolysis, likely reflecting an overall reduction in their ability to produce energy for critical events. Indeed, the ratio between basal ECAR and OCR was similar between the two groups, suggesting that maternal aging does not affect the relative contribution of glycolysis and aerobic metabolism in oocytes.

Cell cleavage after ICSI is another energy requiring event and reflects the ability of the oocyte to process the injected sperm and begin embryonic formation (Altermatt et al., 2009). In agreement with oocyte findings, advanced mare age was associated with impaired mitochondrial function in zygotes that successfully cleaved into two or more cells after ICSI. The ratio of ECAR to OCR was not different between groups and similar to the ratio observed for oocytes, suggesting proportional contribution of aerobic and anaerobic metabolism in MII oocytes and early stage embryos. Cumulus expansion during oocyte maturation represents the end of cumulus cell and oocyte metabolic cooperativity (Collado-Fernandez et al., 2012). After that point, oocytes and early-stage embryos rely on energy produced from internal reserves, such as carboxylic acids (Sutton-McDowall & Thompson, 2015) and fatty acids (Krisher, 2013), as well as substrates obtained from culture media. The reduced aerobic metabolism in embryos derived from old mare oocytes is likely due to impaired mitochondrial capacity, and potentially limited availability of substrates, such as FFA, for oxidative metabolism during this critical time of growth. Other factors, such as enzymatic control of metabolic pathways and cofactors may also be involved, although they were not assessed in the present study.

Maximal oocyte OCR, stimulated by CCCP titrations, is indicative of cellular respiratory capacity and was consistently higher than basal OCR, demonstrating mitochondrial reserve capacity in MII oocytes. Such excess metabolic capacity is seemingly related to the increase in mtDNA copy numbers during oocyte maturation (Hendriks et al., 2015; Lamas-Toranzo et al., 2018) and the cytoplasmic bioenergetic capacity to maintain further embryonic development (Van Blerkom, 2011). Day-2 embryos expressed significantly higher basal OCR and ECAR when compared to basal and maximal values from MII oocytes. When compared to mature oocytes, OCR increases as soon as 9 h after in vitro fertilization for bovine zygotes (Muller et al., 2019) and at the 3- to 4-cell stage for human embryos (Hashimoto et al., 2017). The finding that both OCR and ECAR increased from mature

oocytes to cleavage-stage embryos implies that general metabolic function increases after fertilization. This increase may result, in part, from changes in mitochondrial distribution and morphology or from the recruitment of quiescent mitochondria into active states during early embryogenesis, as described in other species (Bavister & Squirrell, 2000; Bentov et al., 2011; Harvey et al., 2011; Van Blerkom, 2011). An increase in metabolism during the early stages of development is not caused by mitochondrial replication, as this begins at the blastocyst stage in equine embryos (Hendriks et al., 2019).

In our study, we assessed mtDNA numbers to determine if this measurement, often used to estimate mitochondrial numbers, was directly associated with mitochondrial functional assays. In previous studies, equine oocyte mtDNA copy numbers were lower from older when compared to younger mares when assessing oocytes matured in vitro (Rambags et al., 2014). During the first 12 hours of oocyte maturation in vivo, mtDNA copy numbers did not differ over time in young mare oocytes, although a linear decline occurred over time in old mares' oocytes (Campos-Chillon et al., 2015). We found no age difference in mtDNA copy number in MII equine oocytes, and mtDNA was not indicative of mitochondrial function or capacity. Therefore, the lower respiratory capacity of oocytes from old mares in our study may be related to damaged or less active or dysfunctional mitochondria when compared to those in young mare oocytes, rather than reduced overall numbers of mitochondria. Altered mitochondrial morphology, mitochondrial swelling and loss of cristae were more frequently observed in oocytes collected from ovaries harvested from slaughtered older than younger mares after maturation in vitro (Rambags et al., 2014), suggesting that decreases in mitochondrial quality might have contributed to lower OCR in old versus young oocytes. Our results are consistent with a recent study in women that reported negative effects of maternal aging on morulae OCR but not on mtDNA copy numbers (Morimoto et al., 2020).

Mare age did not alter cleavage rates after ICSI, in consonance with previous reports (Altermatt et al., 2009; Frank et al., 2019); however, blastocyst formation at day 7 or 8 after sperm injection was negatively affected by maternal aging. For human embryos, OCR at cleavage stages correlates with viability (Tejera et al., 2012), a finding in agreement with our day-2 embryos. As energy demand and reliance on aerobic metabolism increase during embryonic development (Lane et al., 2001; Gardner & Harvey, 2015; Sanchez et al., 2019), lower blastocyst rates obtained from old mares might be related to reduced metabolic capacity and limited availability of energy substrates originating from their oocytes. Insufficient anaerobic metabolic capacity may also be involved, as oocytes and early embryos from old mares did not compensate for reduced mitochondrial metabolism by increasing anaerobic metabolism.

In conclusion, the metabolic activity and capacity of equine oocytes were impaired by maternal aging. Aerobic metabolism of equine oocytes presumably relies mainly on oxidation of FFA, which were less abundant in oocytes from old than young mares. Insufficient substrates might represent one reason for reduced mitochondrial function and capacity in oocytes from old versus young mares. Oocytes from old mares had limited aerobic and anaerobic metabolism under basal and stimulated conditions, and age-associated alterations were also observed in the metabolic function of ICSI-produced early embryos, with reduced basal aerobic metabolism. These metabolic alterations may contribute to

impaired developmental potential for oocytes from old mares, as observed by their failure to consistently reach the blastocyst stage of development.

Supplementary Material

Refer to Web version on PubMed Central for supplementary material.

Acknowledgements

The authors thank Dr. Rolando Pasquariello for assisting with mtDNA absolute quantification protocols; JoAnne Stokes for performing intracytoplasmic sperm injections; Drs. Jennifer Hatzel, Lisa Maclellan and Fabio Amoroso for assisting with oocyte collections.

Funding

This work was supported by the Cecil and Irene Hylton Foundation, OEDIT Advanced Industries Accelerator POC Program grant, and the National Institute of Health (grant number 1R21HD097601-01).

References

Allen WR, Brown L, Wright M & Wilsher S (2007) Reproductive efficiency of Flatrace and National Hunt Thoroughbred mares and stallions in England. Equine Veterinary Journal 39 438–445. [PubMed: 17910269]

Altermatt JL, Suh TK, Stokes JE & Carnevale EM (2009) Effects of age and equine follicle-stimulating hormone (eFSH) on collection and viability of equine oocytes assessed by morphology and developmental competency after intracytoplasmic sperm injection (ICSI). Reproduction, Fertility and Development 21 615–623.

Barrett SL & Albertini DF (2010) Cumulus cell contact during oocyte maturation in mice regulates meiotic spindle positioning and enhances developmental competence. Journal of Assisted Reproduction and Genetics 27 29–39. [PubMed: 20039198]

Bavister BD & Squirrell JM (2000) Mitochondrial distribution and function in oocytes and early embryos. Human Reproduction 15 189–198.

Bentov Y, Yavorska T, Esfandiari N, Jurisicova A & Casper RF (2011) The contribution of mitochondrial function to reproductive aging. Journal of Assisted Reproduction and Genetics 28 773–783. [PubMed: 21617930]

Brand MD & Nicholls DG (2011) Assessing mitochondrial dysfunction in cells. Biochemical Journal 435 297–312.

Broeckling CD, Afsar FA, Neumann S, Ben-Hur A & Prenni JE (2014) RAMClust: A Novel Feature Clustering Method Enables Spectral-Matching-Based Annotation for Metabolomics Data. Analytical Chemistry 86 6812–6817. [PubMed: 24927477]

Broeckling CD, Ganna A, Layer M, Brown K, Sutton B, Ingelsson E, Peers G & Prenni JE (2016) Enabling Efficient and Confident Annotation of LC–MS Metabolomics Data through MS1 Spectrum and Time Prediction. Analytical Chemistry 88 9226–9234. [PubMed: 27560453]

Campos-Chillon F, Farmerie TA, Bouma GJ, Clay CM & Carnevale EM (2015) Effects of aging on gene expression and mitochondrial DNA in the equine oocyte and follicle cells. Reproduction, Fertility and Development 27 925–933.

Carnevale EM (2008) The mare model for follicular maturation and reproductive aging in the woman. Theriogenology 69 23–30. [PubMed: 17976712]

Carnevale EM (2016) Advances in Collection, Transport and Maturation of Equine Oocytes for Assisted Reproductive Techniques. Veterinary Clinics of North America: Equine Practice 32 379–399.

Carnevale EM & Ginther OJ (1992) Relationships of age to uterine function and reproductive efficiency in mares. Theriogenology 37 1101–1115. [PubMed: 16727108]

Carnevale EM & Ginther OJ (1995) Defective Oocytes as a Cause of Subfertility in Old Mares. Biology of Reproduction 52 209–214.

Carnevale E, Bergfelt D & Ginther O (1993) Aging effects on follicular activity and concentrations of FSH, LH, and progesterone in mares. Animal Reproduction Science 31 287–299.

Carnevale EM, Coutinho da Silva MA, Panzani D, Stokes JE & Squires EL (2005) Factors affecting the success of oocyte transfer in a clinical program for subfertile mares. Theriogenology 64 519–527. [PubMed: 15950272]

Carnevale EM, Maclellan LJ, Ruggeri E & Albertini DF (2012) Meiotic spindle configurations in metaphase II oocytes from young and old mares. Journal of Equine Veterinary Science 32 410–411.

Cecchino GN & Garcia-Velasco JA (2019) Mitochondrial DNA copy number as a predictor of embryo viability. Fertility and Sterility 111 205–211. [PubMed: 30611549]

Cecchino GN, Seli E, Alves da Motta EL & García-Velasco JA (2018) The role of mitochondrial activity in female fertility and assisted reproductive technologies: overview and current insights. Reproductive BioMedicine Online 36 686–697. [PubMed: 29598846]

Chappel S (2013) The Role of Mitochondria from Mature Oocyte to Viable Blastocyst. Obstetrics and Gynecology International 2013 1–10.

Clarke HJ (2018) History, origin, and function of transzonal projections: the bridges of communication between the oocyte and its environment. Animal Reproduction 15 215–223.

del Collado M, da Silveira JC, Sangalli JR, Andrade GM, Sousa LR da S, Silva LA, Meirelles FV & Perecin F (2017) Fatty Acid Binding Protein 3 And Transzonal Projections Are Involved In Lipid Accumulation During In Vitro Maturation Of Bovine Oocytes. Scientific Reports 7 2645. [PubMed: 28572619]

Collado-Fernandez E, Picton HM & Dumollard R (2012) Metabolism throughout follicle and oocyte development in mammals. The International Journal of Developmental Biology 56 799–808. [PubMed: 23417402]

Cuervo-Arango J, Claes AN & Stout TA (2019) A retrospective comparison of the efficiency of different assisted reproductive techniques in the horse, emphasizing the impact of maternal age. Theriogenology 132 36–44. [PubMed: 30986613]

Diez-Juan A, Rubio C, Marin C, Martinez S, Al-Asmar N, Riboldi M, Díaz-Gimeno P, Valbuena D & Simón C (2015) Mitochondrial DNA content as a viability score in human euploid embryos: less is better. Fertility and Sterility 104 534–541.e1. [PubMed: 26051102]

Dumesic DA, Meldrum DR, Katz-Jaffe MG, Krisher RL & Schoolcraft WB (2015) Oocyte environment: follicular fluid and cumulus cells are critical for oocyte health. Fertility and Sterility 103 303–316. [PubMed: 25497448]

Dunning KR, Russell DL & Robker RL (2014) Lipids and oocyte developmental competence: the role of fatty acids and β-oxidation. REPRODUCTION 148 R15–R27. [PubMed: 24760880]

El-Hayek S, Yang Q, Abbassi L, FitzHarris G & Clarke HJ (2018) Mammalian Oocytes Locally Remodel Follicular Architecture to Provide the Foundation for Germline-Soma Communication. Current Biology 28 1124–1131.e3. [PubMed: 29576478]

Frank BL, Doddman CD, Stokes JE & Carnevale EM (2019) Association of equine oocyte and cleavage stage embryo morphology with maternal age and pregnancy after intracytoplasmic sperm injection. Reproduction, Fertility and Development 1812–1822.

Gardner DK & Harvey AJ (2015) Blastocyst metabolism. Reproduction, Fertility and Development 27 638.

Gardner DK & Wale PL (2013) Analysis of metabolism to select viable human embryos for transfer. Fertility and Sterility 99 1062–1072. [PubMed: 23312219]

Harvey A, Gibson T, Lonergan T & Brenner C (2011) Dynamic regulation of mitochondrial function in preimplantation embryos and embryonic stem cells. Mitochondrion 11 829–838. [PubMed: 21168533]

Hashimoto S, Morimoto N, Yamanaka M, Matsumoto H, Yamochi T, Goto H, Inoue M, Nakaoka Y, Shibahara H & Morimoto Y (2017) Quantitative and qualitative changes of mitochondria in human preimplantation embryos. Journal of Assisted Reproduction and Genetics 34 573–580. [PubMed: 28190213]

Hendriks WK, Colleoni S, Galli C, Paris DBBP, Colenbrander B, Roelen BAJ & Stout TAE (2015) Maternal age and in vitro culture affect mitochondrial number and function in equine oocytes and embryos. Reproduction, Fertility and Development 27 957–968.

Hendriks WK, Colleoni S, Galli C, Paris DBBP, Colenbrander B & Stout TAE (2019) Mitochondrial DNA replication is initiated at blastocyst formation in equine embryos. Reproduction, Fertility and Development 31 570–578.

Iwata H, Goto H, Tanaka H, Sakaguchi Y, Kimura K, Kuwayama T & Monji Y (2011) Effect of maternal age on mitochondrial DNA copy number, ATP content and IVF outcome of bovine oocytes. Reproduction, Fertility and Development 23 424–432.

Kameyama Y, Filion F, Yoo JG & Smith LC (2007) Characterization of mitochondrial replication and transcription control during rat early development in vivo and in vitro. Reproduction 133 423–432. [PubMed: 17307910]

Krisher RL (2013) In Vivo and In Vitro Environmental Effects on Mammalian Oocyte Quality. Annual Review of Animal Biosciences 1 393–417. [PubMed: 25387025]

Kushnir VA, Ludaway T, Russ RB, Fields EJ, Koczor C & Lewis W (2012) Reproductive aging is associated with decreased mitochondrial abundance and altered structure in murine oocytes. Journal of Assisted Reproduction and Genetics 29 637–642. [PubMed: 22527902]

Lamas-Toranzo I, Pericuesta E & Bermejo-Álvarez P (2018) Mitochondrial and metabolic adjustments during the final phase of follicular development prior to IVM of bovine oocytes. Theriogenology 119 156–162. [PubMed: 30015144]

Lane M, O'Donovan MK, Squires EL, Seidel GE & Gardner DK (2001) Assessment of metabolism of equine morulae and blastocysts. Molecular Reproduction and Development 59 33–37. [PubMed: 11335944]

Lewis N, Hinrichs K, Leese HJ, McG. Argo C, Brison DR & Sturmey R (2020) Energy metabolism of the equine cumulus oocyte complex during in vitro maturation. Scientific Reports 10 3493. [PubMed: 32103136]

Lopes AS, Greve T & Callesen H (2007) Quantification of embryo quality by respirometry. Theriogenology 67 21–31. [PubMed: 17109946]

May-Panloup P, Chretien M, Malthiery Y & Reynier P (2007) Mitochondrial DNA in the Oocyte and the Developing Embryo. In Current Topics in Developmental Biology, pp 51–83. Elsevier.

Mookerjee SA, Goncalves RLS, Gerencser AA, Nicholls DG & Brand MD (2015) The contributions of respiration and glycolysis to extracellular acid production. Biochimica et Biophysica Acta (BBA) - Bioenergetics 1847 171–181. [PubMed: 25449966]

Morel MCGD, Newcombe JR & Swindlehurst JC (2005) The effect of age on multiple ovulation rates, multiple pregnancy rates and embryonic vesicle diameter in the mare. Theriogenology 63 2482–2493. [PubMed: 15910928]

Morimoto N, Hashimoto S, Yamanaka M, Nakano T, Satoh M, Nakaoka Y, Iwata H, Fukui A, Morimoto Y & Shibahara H (2020) Mitochondrial oxygen consumption rate of human embryos decline with maternal age. Journal of Assisted Reproduction and Genetics 37 1815–1821. [PubMed: 32740687]

Muller B, Lewis N, Adeniyi T, Leese HJ, Brison DR & Sturmey RG (2019) Application of extracellular flux analysis for determining mitochondrial function in mammalian oocytes and early embryos. Scientific Reports 9 16778. [PubMed: 31727902]

Obeidat YM, Evans AJ, Tedjo W, Chicco AJ, Carnevale E & Chen TW (2018) Monitoring oocyte/embryo respiration using electrochemical-based oxygen sensors. Sensors and Actuators B: Chemical 276 72–81.

Obeidat YM, Cheng M-H, Catandi G, Carnevale E, Chicco AJ & Chen TW (2019a) Design of a multi-sensor platform for integrating extracellular acidification rate with multi-metabolite flux measurement for small biological samples. Biosensors and Bioelectronics 133 39–47. [PubMed: 30909011]

Obeidat Y, Catandi G, Carnevale E, Chicco AJ, DeMann A, Field S & Chen T (2019b) A multi-sensor system for measuring bovine embryo metabolism. Biosensors and Bioelectronics 126 615–623. [PubMed: 30508786]

Paczkowski M, Silva E, Schoolcraft WB & Krisher RL (2013) Comparative Importance of Fatty Acid Beta-Oxidation to Nuclear Maturation, Gene Expression, and Glucose Metabolism in Mouse, Bovine, and Porcine Cumulus Oocyte Complexes. Biology of Reproduction 88 1–11. [PubMed: 23288316]

Pasquariello R, Ermisch AF, Silva E, McCormick S, Logsdon D, Barfield JP, Schoolcraft WB & Krisher RL (2019) Alterations in oocyte mitochondrial number and function are related to spindle defects and occur with maternal aging in mice and humans†. Biology of Reproduction 100 971–981. [PubMed: 30476005]

Pirro V, Oliveri P, Ferreira CR, González-Serrano AF, Machaty Z & Cooks RG (2014) Lipid characterization of individual porcine oocytes by dual mode DESI-MS and data fusion. Analytica Chimica Acta 848 51–60. [PubMed: 25263116]

Rambags BPB, van Boxtel DCJ, Tharasanit T, Lenstra JA, Colenbrander B & Stout TAE (2006) Maturation in vitro leads to mitochondrial degeneration in oocytes recovered from aged but not young mares. Animal Reproduction Science 94 359–361.

Rambags BPB, van Boxtel DCJ, Tharasanit T, Lenstra JA, Colenbrander B & Stout TAE (2014) Advancing maternal age predisposes to mitochondrial damage and loss during maturation of equine oocytes in vitro. Theriogenology 81 959–965. [PubMed: 24576711]

Rizzo M, Kops GJPL, Deelen C, Beitsma M, Cristarella S, Stout TAE & de Ruijter-Villani M (2018) Compromised Spindle Assembly Check-point Function in Oocytes From Aged Mares Impairs Correct Chromosome Alignment. Journal of Equine Veterinary Science 66 177.

Rizzo M, Ducheyne KD, Deelen C, Beitsma M, Cristarella S, Quartuccio M, Stout TAE & Ruijter-Villani M (2019) Advanced mare age impairs the ability of in vitro-matured oocytes to correctly align chromosomes on the metaphase plate. Equine Veterinary Journal 51 252–257. [PubMed: 30025174]

Sanchez T, Venturas M, Aghvami SA, Yang X, Fraden S, Sakkas D & Needleman DJ (2019) Combined noninvasive metabolic and spindle imaging as potential tools for embryo and oocyte assessment. Human Reproduction 2349–2361. [PubMed: 31812992]

Simsek-Duran F, Li F, Ford W, Swanson RJ, Jones HW & Castora FJ (2013) Age-Associated Metabolic and Morphologic Changes in Mitochondria of Individual Mouse and Hamster Oocytes. PLoS ONE 8 e64955. [PubMed: 23741435]

Smith CA, Want EJ, O'Maille G, Abagyan R & Siuzdak G (2006) XCMS: Processing Mass Spectrometry Data for Metabolite Profiling Using Nonlinear Peak Alignment, Matching, and Identification. Analytical Chemistry 78 779–787. [PubMed: 16448051]

Sturmey R, Reis A, Leese H & McEvoy T (2009) Role of Fatty Acids in Energy Provision During Oocyte Maturation and Early Embryo Development. Reproduction in Domestic Animals 44 50–58. [PubMed: 19660080]

Su Y-Q, Sugiura K & Eppig J (2009) Mouse Oocyte Control of Granulosa Cell Development and Function: Paracrine Regulation of Cumulus Cell Metabolism. Seminars in Reproductive Medicine 27 032–042.

Sugimura S, Matoba S, Hashiyada Y, Aikawa Y, Ohtake M, Matsuda H, Kobayashi S, Konishi K & Imai K (2012) Oxidative Phosphorylation-linked Respiration in Individual Bovine Oocytes. Journal of Reproduction and Development 58 636–641.

Sutton-McDowall ML & Thompson JG (2015) Metabolism in the pre-implantation oocyte and embryo. Animal Reproduction 12 408–417.

Tejera A, Herrero J, de los Santos MJ, Garrido N, Ramsing N & Meseguer M (2011) Oxygen consumption is a quality marker for human oocyte competence conditioned by ovarian stimulation regimens. Fertility and Sterility 96 618–623.e2. [PubMed: 21782167]

Tejera A, Herrero J, Viloria T, Romero JL, Gamiz P & Meseguer M (2012) Time-dependent O2 consumption patterns determined optimal time ranges for selecting viable human embryos. Fertility and Sterility 98 849–857.e3. [PubMed: 22835446]

TeSlaa T & Teitell MA (2014) Techniques to Monitor Glycolysis. In Methods in Enzymology, pp 91–114. Elsevier.

Van Blerkom J (2011) Mitochondrial function in the human oocyte and embryo and their role in developmental competence. Mitochondrion 11 797–813. [PubMed: 20933103]

Viotti M, Victor AR, Zouves CG & Barnes FL (2017) Is mitochondrial DNA quantitation in blastocyst trophectoderm cells predictive of developmental competence and outcome in clinical IVF? Journal of Assisted Reproduction and Genetics 34 1581–1585. [PubMed: 29080967]

Wang Q, Chi MM, Schedl T & Moley KH (2012) An intercellular pathway for glucose transport into mouse oocytes. American Journal of Physiology. Endocrinology and Metabolism 302 E1511–E1518. [PubMed: 22473000]

Yamanaka M, Hashimoto S, Amo A, Ito-Sasaki T, Abe H & Morimoto Y (2011) Developmental assessment of human vitrified-warmed blastocysts based on oxygen consumption. Human Reproduction 26 3366–3371. [PubMed: 21972254]

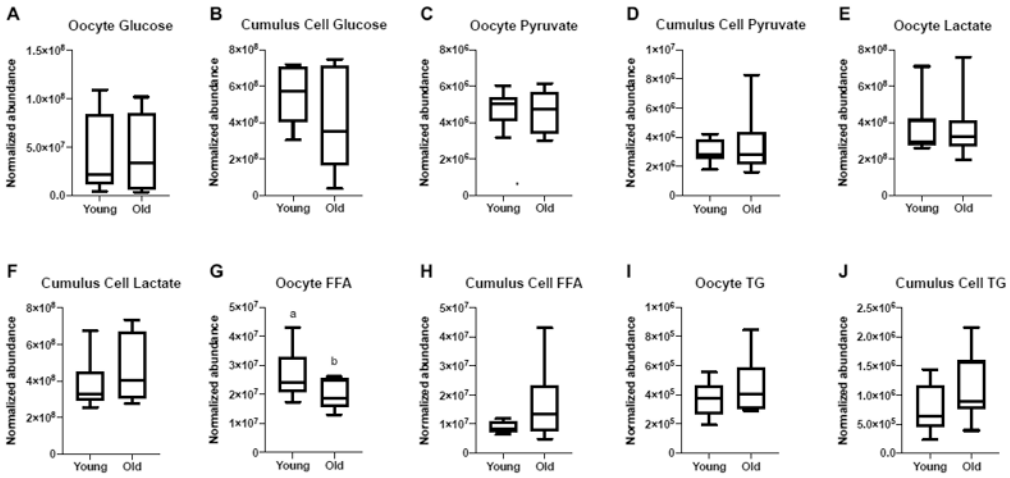

Figure 1. Relative abundance of metabolites in metaphase II oocytes and the respective cumulus cells from young and old mares.

Relative abundance of glucose in (A) oocytes and (B) cumulus cells, pyruvate in (C) oocytes and (D) cumulus cells, lactate in (E) oocytes and (F) cumulus cells, total free fatty acids (FFA) in (G) oocytes and (H) cumulus cells (P=0.08), and total triglycerides (TG) in (I) oocytes and (J) cumulus cells. Single samples were analyzed from Young (n=8 mares) and Old (n=10 mares). Box plots present median, first and third quartiles, with whiskers from minimum to maximum values. Different superscripts indicate differences at $P < 0.05$ (Student's *t* test).

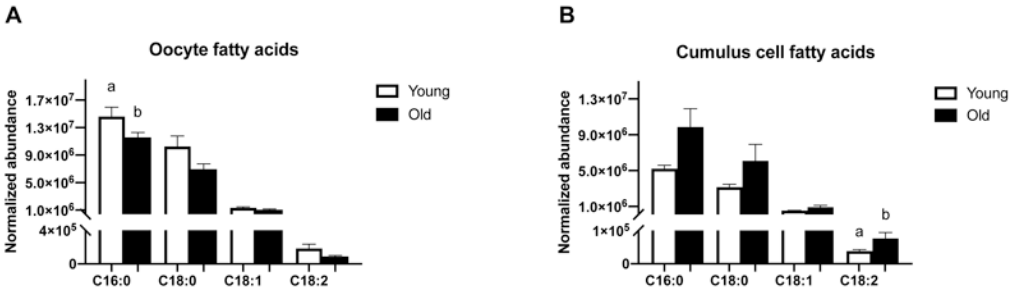

Figure 2. Relative abundance of free fatty acid species in metaphase II oocytes and the respective cumulus cells from young and old mares.

Relative abundance of palmitic acid (C16:0) in (A) oocytes and (B) cumulus cells (P=0.07), stearic acid (C18:0) in (A) oocytes (P=0.06) and (B) cumulus cells, oleic acid (18:1) in (A) oocytes and (B) cumulus cells, and linoleic acid (18:2) in (A) oocytes and (B) cumulus cells. Single samples collected from Young (n=8 mares) and Old (n=10 mares). Barcharts present mean ± SEM. Different superscripts indicate differences at $P < 0.05$ (Student's *t* test and Mann-Whitney test).

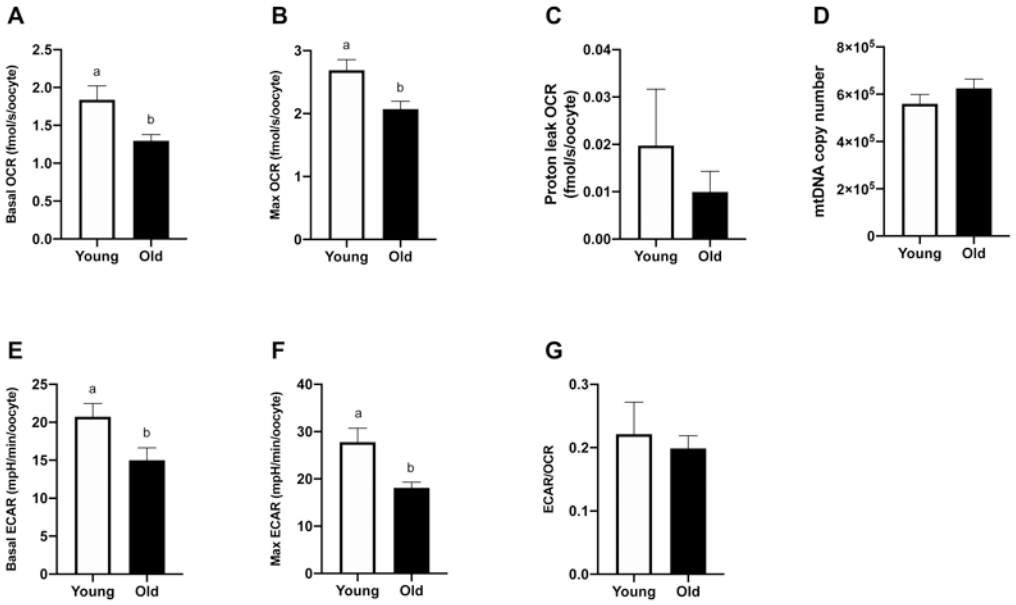

Figure 3. Metabolic function and mitochondrial DNA copy number of metaphase II oocytes from young and old mares.

(A) Basal OCR (Young, n=9 from 7 mares; Old, n=14 from 8 mares), (B) maximal OCR induced by CCCP titrations (Young, n=9 from 7 mares; Old, n=14 from 8 mares), (C) proton leak OCR induced by addition of oligomycin (Young, n=3 from 3 mares; Old, n=7 from 5 mares), (D) mtDNA (Young, n=10 from 7 mares; Old, n=13 from 8 mares), (E) basal ECAR (Young, n=9 from 7 mares; Old, n=14 from 8 mares), (F) maximal ECAR induced by oligomycin titrations (Young, n=3 from 3 mares; Old, n=7 from 5 mares), and (G) proportion of basal glycolytic rate over oxidative phosphorylation rate (Young, n=9 from 7 mares; Old, n=14 from 8 mares). Barcharts present mean ± SEM. Different superscripts indicate differences at $P < 0.05$ (Student's *t* test).

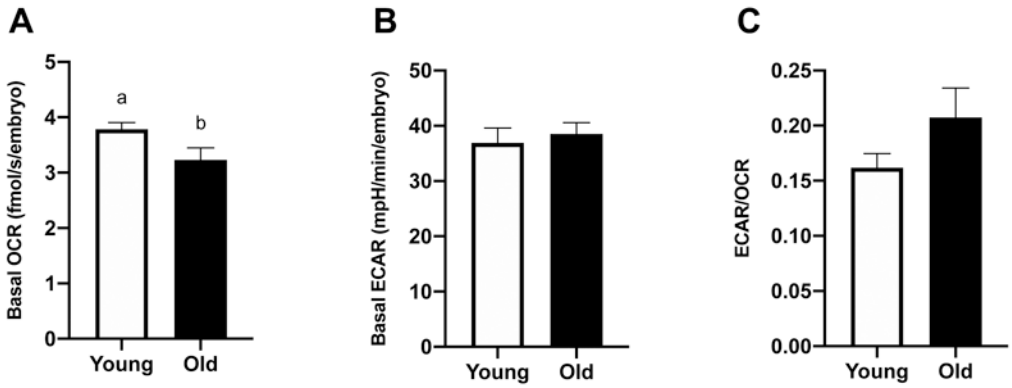

Figure 4. Metabolic function of in vitro-produced, day-2 embryos from young and old mares.
(A) Basal OCR (Young, n=8 from 7 mares; Old, n=10 from 8 mares), (B) basal ECAR (Young, n=7 from 7 mares; Old, n=3 from 3 mares) and (C) proportion of glycolytic rate over oxidative phosphorylation rate (Young, n=7 from 7 mares; Old, n=3 from 3 mares). Barcharts present mean ± SEM. Different superscripts indicate differences at $P < 0.05$ (Student's *t* test).

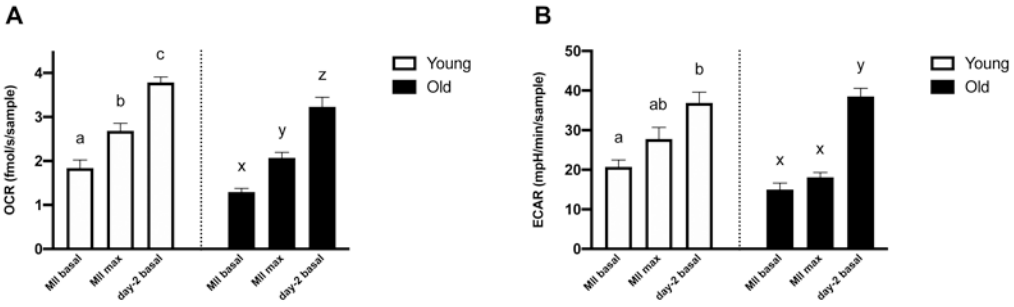

Figure 5. Metabolic function of metaphase II oocytes and in vitro-produced, day-2 embryos compared within the same age group.

(A) Basal and maximal OCR of MII oocytes and basal OCR of day-2 embryos. (B) Basal and maximal ECAR of MII oocytes and basal ECAR of day-2 embryos. Barcharts present mean ± SEM. Different superscripts indicate differences within the same age group (^{abc}Young and ^{xyz}Old) at $P < 0.05$ (one-way ANOVA, post-hoc Tukey's HSD).

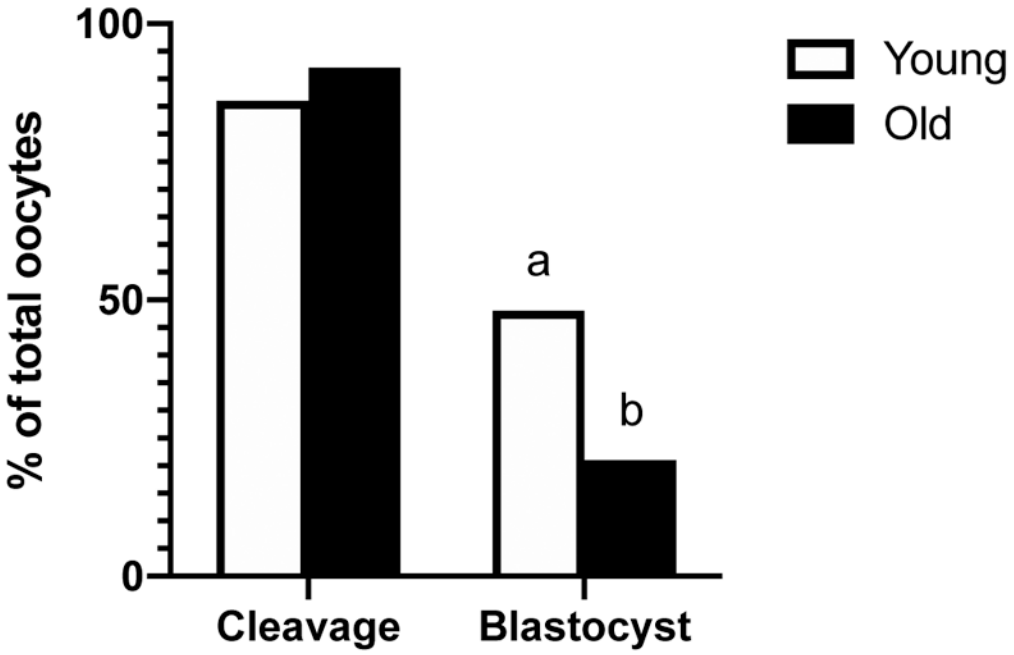

Figure 6. Percentage of sperm injected oocytes that cleaved into at least 2 cells after ICSI (cleavage) and that formed a blastocyst at day 7 or 8 after ICSI.

Cleavage and blastocyst rates of sperm injected oocytes from Young (n=29 oocytes from 13 mares) and Old (n=24 oocytes from 11 mares). Different superscripts indicate differences at $P < 0.05$ for the same end point (Fisher's exact test).